The Journal of Immunology

IL-27 Directly Enhances Germinal Center B Cell Activity and Potentiates Lupus in *Sanroque* Mice

Dipti Vijayan, Norhanani Mohd Redzwan, Danielle T. Avery, Rushika C. Wirasinha, Robert Brink, Giles Walters, Stephen Adelstein, Masao Kobayashi, Paul Gray, Michael Elliott, Melanie Wong, Cecile King, Carola G. Vinuesa, Nico Ghilardi, Cindy S. Ma, Stuart G. Tangye and Marcel Batten

J Immunol 2016; 197:3008-3017; Prepublished online 12 September 2016;
doi: 10.4049/jimmunol.1600652
http://www.jimmunol.org/content/197/8/3008

The Journal of Immunology is published twice each month by
The American Association of Immunologists, Inc.,
9650 Rockville Pike, Bethesda, MD 20814-3994.

Print ISSN: 0022-1767 Online ISSN: 1550-6606.

IL-27 Directly Enhances Germinal Center B Cell Activity and Potentiates Lupus in *Sanroque* Mice

Dipti Vijayan,[*,†,1] Norhanani Mohd Redzwan,[*,2] Danielle T. Avery,[*] Rushika C. Wirasinha,[*,3] Robert Brink,[*,†] Giles Walters,[‡,§,¶] Stephen Adelstein,[‖] Masao Kobayashi,[#] Paul Gray,[**] Michael Elliott,[††,‡‡] Melanie Wong,[§§] Cecile King,[*,†] Carola G. Vinuesa,[‡] Nico Ghilardi,[¶¶] Cindy S. Ma,[*,†] Stuart G. Tangye,[*,†] and Marcel Batten[*,†]

Germinal centers (GC) give rise to high-affinity and long-lived Abs and are critical in immunity and autoimmunity. IL-27 supports GCs by promoting survival and function of T follicular helper cells. We demonstrate that IL-27 also directly enhances GC B cell function. Exposure of naive human B cells to rIL-27 during in vitro activation enhanced their differentiation into $CD20^+CD38^+CD27^{low}CD95^+CD10^+$ cells, consistent with the surface marker phenotype of GC B cells. This effect was inhibited by loss-of-function mutations in *STAT1* but not *STAT3*. To extend these findings, we studied the in vivo effects of IL-27 signals to B cells in the GC-driven $Roquin^{san/san}$ lupus mouse model. $Il27ra^{-/-}Roquin^{san/san}$ mice exhibited significantly reduced GCs, IgG2a(c)$^+$ autoantibodies, and nephritis. Mixed bone marrow chimeras confirmed that IL-27 acts through B cell– and $CD4^+$ T cell–intrinsic mechanisms to support GCs and alter the production of pathogenic Ig isotypes. To our knowledge, our data provide the first evidence that IL-27 signals directly to B cells promote GCs and support the role of IL-27 in lupus. ***The Journal of Immunology*****, 2016, 197: 3008–3017.**

Germinal centers (GCs) are temporary microstructures that form within lymphoid tissues to facilitate the cellular interactions required for successful T cell–dependent humoral responses. GCs are required for affinity maturation of Abs and the generation of B cell memory. During the process of affinity maturation, B cells undergo somatic hypermutation of the BCR, a process that yields new Ag specificities. This process also has the potential to generate self-reactive clones (1) and, therefore, is tightly regulated. Although GCs are dedicated to the improvement of B cell responses to Ag, other cell types are also critical for this process. For example, follicular dendritic cells are specialized APCs in GCs, and $CD4^+$ T follicular helper (T_{FH}) cells are essential for the selection of B cells with improved affinity for Ag (2). Dysregulated GCs can lead to the development of autoimmune pathologies, particularly lupus and other autoantibody-mediated diseases (2, 3). Therefore, understanding the factors that promote, guide, and regulate GC reactions are critical to understanding B cell–mediated autoimmune diseases.

IL-27, a heterodimeric cytokine comprising the IL-27p28 and EBI3 subunits, is a member of the IL-12/IL-6 family of cytokines and can exert pro- and anti-inflammatory effects during immune responses (4–8). Most studies of IL-27 focused on its effects on T cells. Importantly, there is evidence that IL-27 can support Ab-driven autoimmune disease: IL-27 is significantly elevated in sera of untreated systemic lupus erythematosus (SLE) patients (9, 10), and several studies revealed an essential role for IL-27 in murine lupus and proteoglycan-induced arthritis (11–14). Although IL-27 was shown to be important for GCs, only indirect effects of IL-27

*Immunology Division, Garvan Institute of Medical Research, Darlinghurst, New South Wales 2010, Australia; [†]St. Vincent's Clinical School, University of New South Wales, Sydney, New South Wales 2052, Australia; [‡]Department of Immunology and Infectious Disease, John Curtin School of Medical Research, Australian National University, Canberra, Australian Capital Territory 2601, Australia; [§]Department of Renal Medicine, Canberra Hospital, Canberra, Australian Capital Territory 2605, Australia; [¶]Australian National University Medical School, Canberra, Australian Capital Territory 2601, Australia; [‖]Clinical Immunology, Royal Prince Alfred Hospital, Sydney, New South Wales 2050, Australia; [#]Department of Pediatrics, Hiroshima University Graduate School of Biomedical Sciences, Hiroshima 734-8553, Japan; [**]University of New South Wales School of Women's and Children's Health, Sydney, New South Wales 2031, Australia; [††]Sydney Medical School, University of Sydney, Sydney, New South Wales 2006, Australia; [‡‡]Chris O'Brien Lifehouse Cancer Centre, Royal Prince Alfred Hospital, Sydney, New South Wales 2050, Australia; [§§]Children's Hospital at Westmead, Westmead, New South Wales 2145, Australia; and [¶¶]Department of Immunology, Genentech Inc., South San Francisco, CA 94080

[1]Current address: QIMR Berghofer Medical Research Institute, Brisbane, Australia.

[2]Current address: Department of Immunology, School of Medical Sciences, University of Science, Malaysia Health Campus, Kubang Kerian, Kelantan, Malaysia.

[3]Current address: Department of Biochemistry and Molecular Biology, Monash University, Clayton, Victoria, Australia.

ORCIDs: 0000-0002-5710-4009 (N.M.R.); 0000-0003-4854-9353 (G.W.); 0000-0001-7221-6298 (S.A.); 0000-0002-2001-822X (M.K.); 0000-0001-9799-0298 (C.G.V.); 0000-0003-4945-3097 (N.G.); 0000-0002-5360-5180 (S.G.T.).

Received for publication April 14, 2016. Accepted for publication August 9, 2016.

This work was supported primarily by a research grant from the National Health and Medical Research Council of Australia (GNT1008558). It was also supported by other research fellowships and grants from the National Health and Medical Research Council (to M.B., C.S.M., R.B., C.K., C.G.V., and S.G.T.). S.G.T. is a Fulbright Senior Scholar.

M.B. and D.V. designed the studies and wrote the manuscript; M.B., D.V., R.B., C.K., S.G.T., N.G., and C.S.M. participated in experimental design; D.V., N.M.R., D.T.A., and R.C.W. conducted experiments; D.V., N.M.R., and M.B. analyzed the data; G.W. did mouse pathology assessment; S.A., M.K., P.G., and M.W. provided primary immunodeficiency patient blood; and M.E., C.G.V., N.G., C.S.M., and S.G.T. provided reagents, cells, and/or mice.

Address correspondence and reprint requests to Dr. Marcel Batten, Garvan Institute of Medical Research, 384 Victoria Street, Darlinghurst, NSW 2010, Australia. E-mail address: m.batten@garvan.org.au

The online version of this article contains supplemental material.

Abbreviations used in this article: BM, bone marrow; GC, germinal center; MFI, mean fluorescence intensity; rh, recombinant human; SLE, systemic lupus erythematosus; T_{FH}, T follicular helper.

on GC B cells were described. For example, IL-27 supports IL-21 production by, and survival of, T_{FH} cells in mice (11, 15, 16) and differentiation of IL-21–producing human T_{FH} cells in vitro (17, 18), which, in turn, supports the GC B cell response. Despite this, it is not known whether IL-27 signals directly to B cells are required for normal GC activity.

B cells express the complete IL-27R, which is detected on human resting plasma, naive, and memory B cells, and it is upregulated on CD40-stimulated naive, memory, and GC B cells (19, 20). IL-27 activates STAT1 and STAT3 and induces T-bet expression in human and mouse B cells in vitro (20, 21). In murine B cell cultures, IL-27 directly promoted Ig class switching to IgG2a, while inhibiting switching to IgG1, through T-bet and STAT1 (21). Consistent with this, *Il27ra*$^{-/-}$ mice have reduced basal serum IgG2a (IgG2c on the B6 genetic background), but other serum total Ig titers are unaffected (22). Apart from this possible effect on class switching, the biological significance of IL-27Ra expression on B cells during an in vivo immune response is unknown.

In this study, we investigated how IL-27 directly influences human and mouse B cells with respect to GC activity. *Sanroque* (*Roquin*$^{san/san}$) mice represent an ideal system to study the importance of IL-27 for GC B cells and Ab-mediated autoimmune disease in vivo. *Roquin*$^{san/san}$ mice develop spontaneous GCs and autoimmune pathology (23–25) as the result of a single ENU-induced mutation in the *Roquin1*/*Rc3h1* gene (23). *Roquin1* is an RNA-binding RING-type E3 ubiquitin ligase that regulates the stability of mRNAs encoding proteins central to GC function, including ICOS, OX40, IFN-γ, and TNF (26–29). *Roquin*$^{san/san}$ mice develop splenomegaly, serum autoantibodies, and immune complex deposition in the kidney, leading to pathology characteristic of glomerulonephritis (23). IL-27 was found to induce phenotypic characteristics of GCs in human B cells. Furthermore, *Il27ra*$^{-/-}$*Roquin*$^{san/san}$ mice developed fewer GC B cells and less severe disease than *Roquin*$^{san/san}$ mice, revealing the physiological relevance of IL-27 to GC biology. Lastly, using a bone marrow (BM) chimeric approach, we confirmed a B cell–intrinsic effect of IL-27 in this process. Together, our findings point to a previously unappreciated in vivo role for IL-27 signaling to B cells in directing T cell–dependent B cell responses.

Materials and Methods

Human tissue samples

Human buffy coats were obtained from the Australian Red Cross Blood Service. Tonsillar tissues were collected from patients undergoing tonsillectomy (Mater Hospital, North Sydney, Australia). Peripheral blood was also collected from patients with loss-of-function mutations in *STAT1* ($STAT1_{MUT}$; STAT1-Y701C; two donors with STAT1-G250E) and *STAT3* ($STAT3_{MUT}$; STAT3-V637M; STAT3-V432M; STAT3-F621L). Approval for this study was obtained from the human research ethics committees of the St. Vincent's Hospital and Sydney South West Area Health Service (Australia).

Mice

Il27ra$^{+/+}$*Roquin*$^{san/san}$, *Il27ra*$^{-/-}$*Roquin*$^{san/san}$, CD45.1 congenic *Roquin*$^{san/san}$, *Il27ra*$^{+/+}$, *Il27ra*$^{-/-}$ (C57BL6 background >35 generations), and C57BL/6 mice were bred in a specific pathogen–free facility at Australian BioResources (Moss Vale, Australia). *Rag1*$^{-/-}$ animals were purchased from the Animal Resources Centre (Perth, Australia). All animal procedures were approved by the Institutional Animal Care and Use Committee at The Garvan Institute/St. Vincent's Animal Experimentation Ethics Committee.

For in vivo cytokine analysis, *Il27ra*$^{+/+}$*Roquin*$^{san/san}$ and *Il27ra*$^{-/-}$*Roquin*$^{san/san}$ mice were administered brefeldin A (25 μg i.v.) 6 h prior to tissue harvest.

Abs, cytokines, and flow cytometry

For stimulation assays, recombinant cytokines recombinant human (rh) IL-27, rhIL-21, and recombinant mouse IL-27 were purchased from eBioscience, PeproTech, and R&D Systems, respectively. Flow cytometric staining was performed using the following panel of anti-human Abs: CD10, CD20, CD27, Bcl-6 (all from BD Biosciences), CD38 (eBioscience), CD95 (BioLegend), and IL-27Rα (R&D Systems; Mouse IgG_{2B} Clone 191106). The following anti-mouse antibodies were used: GL-7, CD95, B220, ICOS, PD-1, CXCR5, CD138, IgG2a(c), IgG1 (all from BD Biosciences), CD4 (eBioscience), and CD38 (BioLegend). Briefly, cells were stained with the desired surface markers for 30 min on ice. For intracellular staining, cells were stained first with surface markers, followed by fixation and permeabilization using fixation-permeabilization buffer (eBioscience). Flow cytometry data were acquired on a BD FACSCanto II cytometer and analyzed using FlowJo v10 software (TreeStar).

B cell isolation and in vitro cytokine stimulation

Human PBMCs were labeled with mAbs against CD10-allophycocyanin, CD20-allophycocyanin Cy7, and CD27 PECy7. Naive B cells ($CD10^-$ $CD20^+CD27^-IgG^-$) were sorted on a FACSAria III (BD Biosciences). Tonsillar mononuclear cells were labeled with mAbs against CD20, CD27, and CD38 to isolate naive ($CD20^+CD27^-CD38^-$), memory ($CD20^+CD27^+$ $CD38^-$), and GC ($CD20^{hi}CD27^{int}D38^{hi}$) B cells (FACSAria III; BD Biosciences). The purity of the recovered populations was >98%.

Isolated B cells from healthy donors or $STAT3_{MUT}$ or $STAT1_{MUT}$ patients were cultured at 50–100 × 10^3 cells/well in a 96-well U-bottom plate with 2.5 μg/ml $F(ab')_2$ fragment of goat anti-human IgM/G/A (Jackson ImmunoResearch) and CD40L [prepared in-house and used as described previously (30) or purchased from R&D Systems and used at 0.8 μg/ml], alone or together with 100 ng/ml IL-27 (R&D Systems) or 50 ng/ml IL-21 (PeproTech). Differentiation of B cells was assessed using a panel of markers: Bcl-6-PE, CD38-PerCp Cy5.5, CD20-allophycocyanin Cy7, CD27-PECy7, CD10-allophycocyanin, CD95-BV421, and IL-27Ra-PE. Isolated naive and memory B cells were labeled with the proliferation dye CFSE (eBioscience) prior to culture. Absolute counts were also determined by adding Calibrite beads to the cells just before data acquisition on a BD FACSCanto II flow cytometer (both from BD Biosciences).

Real-time RT-PCR

For relative quantitation of *IL27ra* mRNA, total RNA was isolated from unstimulated FACS-sorted cells or FACS-sorted cells that were stimulated for 48 h with anti-human IgM/G/A and CD40L using an RNeasy Mini Kit (QIAGEN). Quantitative RT-PCR was performed using the Roche Universal Probe Library system and a Roche LightCycler 480 instrument. For each sample, duplicate test reactions and control reactions lacking reverse transcriptase were analyzed for expression of *IL27ra* using intron-spanning primer sets; results were normalized to those of the housekeeping ribosomal protein (RP) L13A mRNA. Arbitrary units given are the fold change relative to *RPL13A* and multiplied by 10,000. Primer sequences are as follows: *IL27Ra* (forward 5′-CCCCCTCCGAGTTACACC-3′ and reverse 5′-ACTGCCACAGTCTGGGTTTT-3′, UPL probe #21) and *RPL13A* (forward 5′-CAAGCGGATGAACACCAAC-3′ and reverse 5′-TGTGGGGCAGCATACCTC-3′, UPL probe #28).

Generation of BM chimeras

Rag1$^{-/-}$ recipient mice were sublethally irradiated with 500 rad 1 d before reconstitution, via i.v. injection, with a total of 2.5 × 10^6 BM cells, consisting of equal numbers of lineage-negative cells from CD45.1 *Il27ra*$^{+/+}$*Roquin*$^{san/san}$ and CD45.2 *Il27ra*$^{-/-}$*Roquin*$^{san/san}$ mice. The chimeric mice were maintained on antibiotics for 6 wk postreconstitution. Tissues were harvested at week 15 postreconstitution, and flow cytometric analysis of cellular populations was performed.

Renal histology

Kidneys were harvested from *Il27ra*$^{+/+}$*Roquin*$^{san/san}$ and *Il27ra*$^{-/-}$ *Roquin*$^{san/san}$ mice of various ages and fixed in 10% formalin solution at room temperature overnight. Thereafter, tissues were placed in 70% ethanol prior to paraffin embedding. Kidney sections were cut to 4 μm thickness and stained with H&E. Nephritis scores were blindly evaluated by a clinical pathologist, using a scoring system of 0–4, to individually rate glomeruli damage, vasculitis, and tubulointerstitial damage, as described previously (25). Scores were added to give a total renal damage score.

For analysis of immune complex deposition, kidneys were frozen in OCT, sectioned to 4 μm thickness, and stained by immunofluorescence using rat anti-mouse IgG1-FITC and biotin-labeled rat anti-mouse IgG2a (c) that was streptavidin conjugated to Alexa Fluor 350. Semi-quantitative analysis of immune complex deposition was evaluated using Leica software. Briefly, a region of interest around each glomerulus was marked, and the positive pixel/area within that region of interest was determined. A

positive pixel/area was also calculated for a glomerulus that was negative for IgG staining. This was considered as background. The Gray Value for IgG immune complex deposition was calculated as: (pixel/area for IgG+ glomerulus)/(pixel/area for background fluorescence in the same section). Seven or eight glomeruli were assessed per mouse.

Serum anti-dsDNA Ab ELISA

Sera were collected after cardiac puncture bleed from groups of mice aged 13–15 and 19–21 wk. Briefly, anti-dsDNA Abs in mouse sera were detected by coating plates with 10 mg/ml methylated BSA (Sigma-Aldrich) overnight, followed by 5 mg/ml genomic DNA from calf thymus (Sigma-Aldrich) for ≥2 h. The genomic DNA was sheared by sonication, followed by digestion with S1 nuclease (Promega). Sera were added at a dilution of 1:20, followed by the addition of 100 μl of HRP-conjugated goat anti-mouse IgG2c or IgG1 and a 30-min incubation. Finally, 100 μl of 3,3′,5,5′-tetramethylbenzidine substrate was added and incubated for 15 min in the dark prior to adding the stop solution. Plates were read at 405 nm using a BioTek Plate reader. Serum obtained from a positive control of *Roquin*$^{san/san}$ was used to construct a standard curve and assigned a concentration of 100 so that other sera could be given a relative concentration. The same positive control serum was used across all plates.

Statistical analysis

Statistical differences between two datasets were determined using the unpaired Student *t* test for comparison of unlinked groups or the paired *t* test for linked samples (human B cells from the same donor with different cytokine treatments or CD45.1 and CD45.2 populations within the same host chimeric mouse). The Mann–Whitney nonparametric *U* test was used where indicated Prism; GraphPad Software).

Results

IL-27 promotes the differentiation of human B cells with cell surface markers characteristic of GC B cells via STAT1 activation

We first investigated the effect of rhIL-27 on isolated human B cells during in vitro activation. A combination of CD40L and anti-Ig (BCR cross-linking) was selected for activation because these combined signals were shown to promote the generation of cells with features of GC B cells from naive precursors (31). Naive B cells ($CD10^-CD20^+CD27^-IgG^-$) were purified from PBMCs and stimulated with CD40L and anti-Ig Abs in the presence or absence of rhIL-27 for 72 h. Expression of surface markers that delineate differentiated B cells was assessed using flow cytometry. B cell subset gates were defined according to unsorted and unstimulated tonsil cell preparations, which were analyzed concurrently (Fig. 1A). When FACS-purified peripheral blood naive B cells (Fig. 1A) were stimulated in vitro, the addition of rhIL-27 consistently enhanced the proportion of cells acquiring a $CD20^+CD38^+$ phenotype compared with cells treated with CD40L/anti-Ig alone (Fig. 1B). The average induction of $CD20^+CD38^+$ cells in the presence of IL-27 was 2.37 ± 1.3-fold greater than for cells stimulated with CD40 and anti-Ig alone (Fig. 1C). To determine whether the in vitro–induced $CD20^+CD38^+$ B cells were similar to GC B cells in terms of other cell surface markers, we compared expression of CD10, CD95 (Fas), and CD27 on these cells with naive B cells and bona fide tonsillar GC B and memory B cells. In line with the cell surface marker phenotype of GC B cells, stimulated cells that became $CD38^+$ were also $CD10^+$, $CD95^+$, and $CD27^{lo}$ (Fig. 1D). The mean fluorescence intensity (MFI) of CD27 was slightly higher on some stimulated samples compared with GC B cells but remained low compared with tonsillar memory cells (Fig. 1D). These data suggest that, during the activation of human naive B cells, IL-27 promotes the development of B cells that coexpress CD38, CD95, and CD10, reminiscent of GC B cells present in human lymphoid tissue.

IL-27 significantly increased expression of CD95 on CD40L/anti-Ig–stimulated naive human B cells at 72 h poststimulation (Fig. 1D, Supplemental Fig. 1A, 1B), consistent with a previous report (20). Although IL-27 altered CD95 expression, it had no effect on cell recovery (Supplemental Fig. 1C). B cell proliferation was similar in the presence or absence of IL-27 (Supplemental Fig. 1D). These data suggest that CD95 upregulation was not the result of changes in cell death or proliferation; rather, elevated CD95 levels reflect the ability of IL-27 to induce an altered differentiation program in B cell cultures.

In our experiments, we observed an early, but transient, induction of Bcl-6 after anti-Ig/CD40L stimulation of naive or memory B cells at 24 h, followed by loss of expression by 72 h. Rapid loss of Bcl-6 expression was observed even when sorted tonsillar GC B cells were cultured under similar conditions (Supplemental Fig. 1E). Together, these data suggest that the requirements for maintenance of Bcl-6 were unavailable in our in vitro culture system. Therefore, we could not discern any influence of IL-27 on Bcl-6 levels (Supplemental Fig. 1E, 1F).

Memory B cells have different thresholds for activation and differentiation compared with naive cells (32). Therefore, we examined the effect of rhIL-27 on memory B cells during restimulation. For these experiments, memory ($CD20^+CD38^-CD27^+$) and naive ($CD20^+CD38^-CD27^-$) B cells were isolated from human tonsils, and the dynamics of B cell differentiation in response to rhIL-27 stimulation were examined. As observed for B cells isolated from peripheral blood, rhIL-27 significantly enhanced the differentiation of tonsillar naive B cells toward a $CD38^+CD20^{hi}$ phenotype at 72 h (Supplemental Fig. 1G; average 4.12-fold increase) with a similar, although nonsignificant, enhancement noted after 5 d ($p = 0.0551$). rhIL-27 also significantly enhanced $CD38^+CD20^{hi}$ B cell differentiation from stimulated memory B cells at 72 h and 5 d, although the magnitude of the enhancement was less than that observed for naive B cells (Supplemental Fig. 1G; average 1.57-fold and 1.41-fold, respectively). These data are in line with previous observations that naive and memory human B cells express comparable levels of IL-27Rα, but memory cells respond relatively poorly to the stimulatory effects of rhIL-27 (20).

We next assessed whether addition of rhIL-27 could induce B cell differentiation to Ab-secreting cells. Activation of B cells by CD40L and rhIL-21 leads to STAT3-dependent differentiation into plasmablasts (30). Therefore, we stimulated sorted naive, memory, or GC B cells with CD40L and assessed plasmablast differentiation at day 5 in the absence and presence of IL-27, IL-21, or both. As expected, rhIL-21 resulted in the emergence of a robust $CD38^{hi}CD20^{lo}CD27^{hi}$ plasmablast population in all three B cell subpopulations. In contrast, there was no induction of plasmablast differentiation by rhIL-27 (Supplemental Fig. 2A–C). The addition of both cytokines to cultures of CD40L-stimulated B cells resembled the effects of rhIL-21 alone, indicating that rhIL-27 has no cooperative effect on IL-21–induced plasmablast generation from human B cells (Supplemental Fig. 2D). In fact, coadministration of rhIL-27 caused a diminution of plasmablast percentages in two of five donors (one donor is represented in Supplemental Fig. 2A–C). Consistent with the FACS data, we observed increased secretion of IgG, IgM, and IgA in cultures of CD40L-stimulated B cells treated with rhIL-21 but not rhIL-27 (Supplemental Fig. 2E–H).

STAT1 and STAT3 are two major signal transducers downstream of IL-27R (4). To determine which pathway facilitated IL-27R–induced B cell differentiation, we examined naive B cells isolated from patients with disease-causing loss-of-function mutations in *STAT1* or *STAT3*. The ability of rhIL-27 to enhance differentiation of human naive $STAT3_{MUT}$ B cells into $CD20^+CD38^+$ B cells was similar to that observed for normal naive B cells (2.37 ± 1.3-fold and 2.71 ± 1.02-fold,

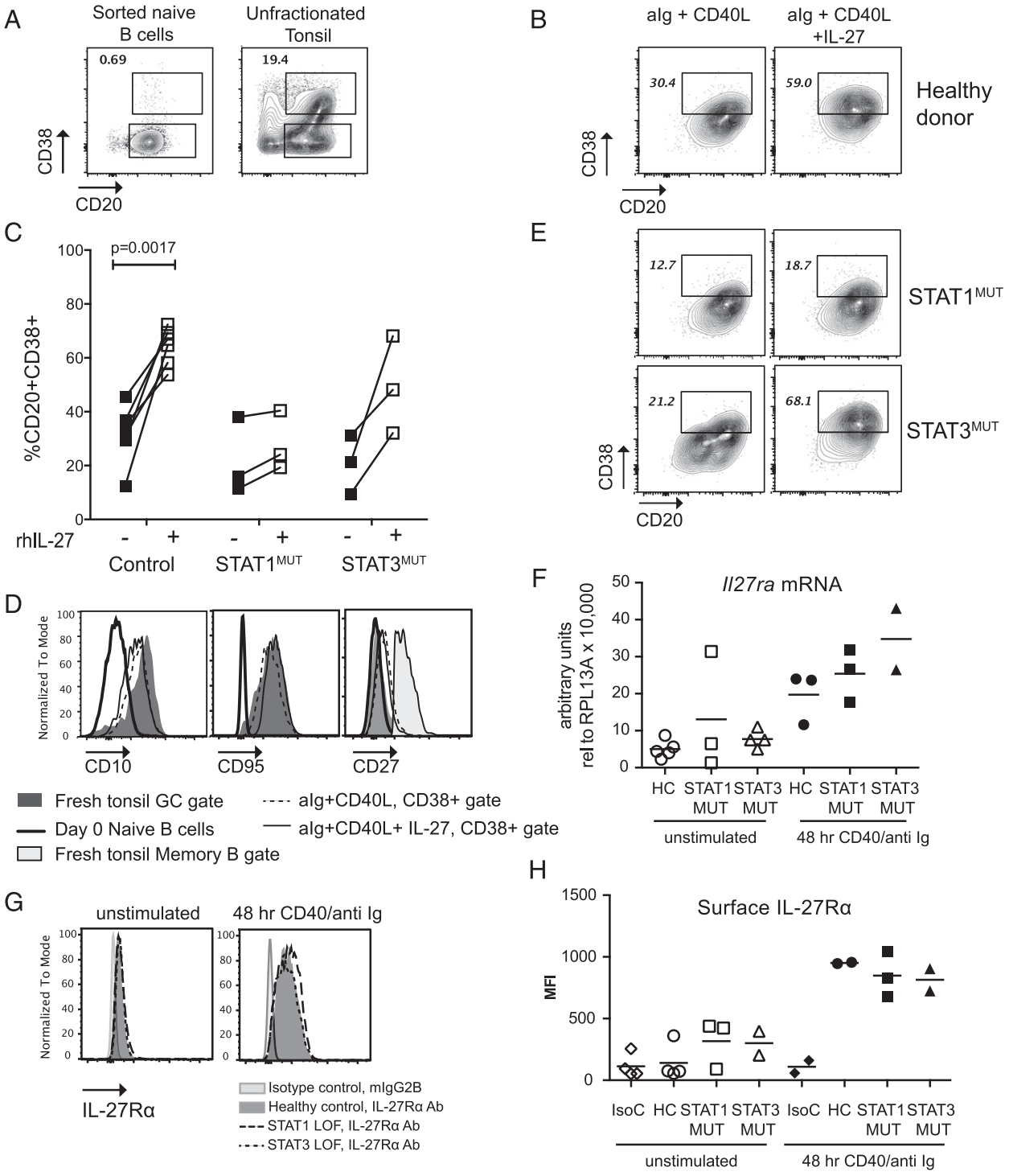

FIGURE 1. IL-27 induces STAT1-dependent differentiation of human GC-like B cells. Naive B cells ($CD20^+$, $CD27^-$, $CD38^-$) purified from PBMCs of healthy donors or patients with *STAT1* or *STAT3* loss-of-function mutations were stimulated with CD40L/anti-Ig in the absence (−) or presence (+) of rhIL-27. The cells were stained with Abs against CD20, CD38, CD95, CD10, CD27 and IL-27Ra. (**A**) Representative CD38 versus CD20 plots for sorted naive PBMCs (left panel) along with unfractionated tonsil cells, which were stained concurrently to define B cell population gates (right panel). $CD38^{hi}CD20^{hi}$ cells reflecting the GC B cells in tonsil are gated. (**B**) Representative CD38 versus CD20 plots for sorted naive B cells from healthy donors after a 72-h stimulation in the presence or absence of rhIL-27. (**C**) The percentage of cells in the $CD38^+CD20^+$ gate was quantitated for multiple donors. Each symbol represents an individual donor, and cells from the same donor are connected by a line. Donor responses were assessed as independent experiments. The paired *t* test was used to compare cells stimulated in the absence and presence of rhIL-27. (**D**) CD10, CD95, and CD27 levels on the $CD38^+CD20^+$ gate of stimulated cells (thin and dashed lines, as indicated) were compared with levels in unstimulated naive B cells (thick black line) and tonsillar GC B cells (dark gray shading). For CD27 (far right panel), a tonsil memory B cell gate is included for comparison (light gray shading). (**E**) Representative CD38 versus CD20 plots for naive B cells sorted from *STAT1* or *STAT3* loss-of-function patient PBMCs and stimulated for 72 h in the presence or absence of rhIL-27. (**F**) Relative *Il27ra* mRNA levels in unstimulated naive B cells or those stimulated for 48 h with CD40 and anti-Ig were determined by real-time RT-PCR. Each symbol represents an individual donor. (**G** and **H**) Naive or stimulated B cells, as in (F), were stained with anti–IL-27Rα Ab. (G) Representative graphs. (H) MFI of IL-27Rα for multiple donors compared with mouse IgG2B isotype control stained healthy control (HC) B cells. Each symbol represents an individual donor. Horizontal lines represent the means.

respectively, compared with CD40L/anti-Ig alone; Fig. 1C, 1E). Again, the cells in the $CD20^+CD38^+$ gate were also $CD10^+CD95^+CD27^{lo}$ (data not shown). However, this effect of rhIL-27 was greatly reduced in $STAT1_{MUT}$ B cells (1.42 ± 0.32-fold increase compared with CD40L/anti-Ig alone; Fig. 1C, 1E). Likewise, CD95 upregulation by IL-27 was observed in healthy control (1.87 ± 0.40-fold) and $STAT3_{MUT}$ (2.26 ± 0.52-fold) cells but not in $STAT1_{MUT}$ B cells (1.07 ± 0.11-fold; Supplemental Fig. 1B). This defect was not due to lack of IL-27R expression on $STAT1_{MUT}$ cells, as indicated by comparable levels of *IL27RA* mRNA and IL-27Rα protein on the surface of naive B cells from healthy controls and STAT1-deficient individuals (Fig. 1F–H). Thus, the effect of IL-27 on B cell differentiation is STAT1 dependent. Together, the data indicate that STAT1 signaling downstream of IL-27R activation specifically promotes the generation of $CD20^{hi}CD38^+CD10^+CD95^+CD27^{lo}$ B cells, but not plasmablasts, from naive precursors.

GC defects in $Il27ra^{-/-}Roquin^{san/san}$ *mice*

The data obtained from IL-27–treated human B cells in vitro suggested that IL-27 could directly promote expression of cell surface markers associated with GC B cells. However, the lack of Bcl-6 expression, even in sorted and cultured tonsil GC B cells, indicated that complete GC differentiation could not be achieved in vitro. Therefore, we next focused on understanding the significance of IL-27 in directing GC differentiation in vivo by using *Roquin*$^{san/san}$ mice as a model of spontaneous GCs and autoimmunity. Consistent with other lupus models (11–14), the overall kidney pathology determined on the basis of the glomerular and tubulointerstitial nephritis was significantly reduced in the absence of IL-27 signaling in 19–21-wk-old female mice (Fig. 2A, 2B). The levels of vasculitis in kidney were low in both groups, with two of seven wild-type and two of five knockout mice scoring positive (data not shown). $Il27ra^{-/-}Roquin^{san/san}$ mice also displayed significantly ameliorated splenomegaly compared with $Il27ra^{+/+}Roquin^{san/san}$ mice (Fig. 2C), although the spleens remained large compared with healthy $Il27ra^{+/+}$ or $Il27ra^{-/-}$ control mice.

Lymphocyte populations were assessed in groups of *Il27ra*-sufficient and -deficient *Roquin*$^{san/san}$ mice at 13–15 wk of age. Lower overall splenocyte numbers were observed in $Il27ra^{-/-}Roquin^{san/san}$ mice compared with $Il27ra^{+/+}Roquin^{san/san}$ mice (Fig. 2D). In line with our previous studies in adjuvant-induced GC systems (11), the percentage and number of $CD4^+CXCR5^+PD1^+$ T_{FH} cells (Supplemental Fig. 3A) and $B220^+GL7^+CD38^{lo}$ GC B cells (Fig. 2F, 2G) were reduced significantly in the absence of IL-27 signaling. For those GC B cells that were present in each group of mice, the percentages of light zone ($CXCR4^{lo}CD86^+$) and dark zone ($CXCR4^{hi}CD86^{lo}$) GC B cells in $Il27ra^{+/+}Roquin^{san/san}$ and $Il27ra^{-/-}Roquin^{san/san}$ mice were comparable (Supplemental Fig. 3B, 3C). The percentage of

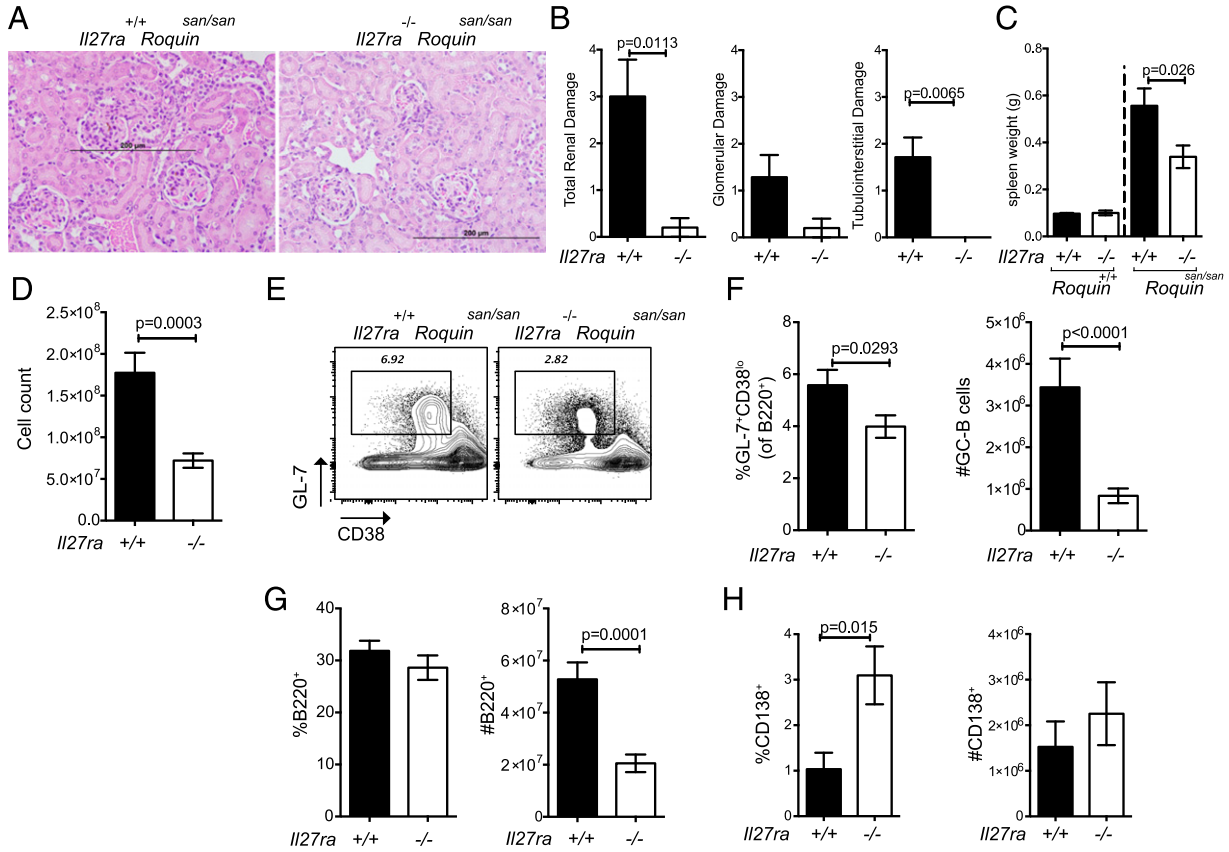

FIGURE 2. GC defects in $Il27ra^{-/-}Roquin^{san/san}$ mice. (**A**–**C**) Groups of 19–21-wk-old female mice were euthanized and assessed for renal pathology and splenomegaly. (A) Representative images of renal damage in the kidneys of $Il27ra^{+/+}Roquin^{san/san}$ and $Il27ra^{-/-}Roquin^{san/san}$ mice, as determined by H&E staining. Scale bars, 200 μm. (B) Renal scores of cumulative renal damage (left panel) and individual glomerular and tubulointerstitial damage (right panel) ($n = 4-8$). (C) Spleen weights in groups of female $Il27ra^{+/+}Roquin^{san/san}$ and $Il27ra^{-/-}Roquin^{san/san}$ mice ($n = 10$) compared with $Roquin^{+/+}$ healthy controls (10–12 wk). (**D**–**H**) Splenocytes were isolated from $Il27ra^{+/+}Roquin^{san/san}$ and $Il27ra^{-/-}Roquin^{san/san}$ mice at ages 13–15 wk, and cell populations were assessed by flow cytometry. (D) Total splenocyte cell counts (n = 19–21). (E) Representative analysis of GC B cell staining ($GL\text{-}7^+CD38^{lo}$ cells, pregated on $B220^+$). (F) Percentages and absolute cell counts per spleen for GC B cells. (G) Percentages and cell counts for total $B220^+$ B cells. (H) Percentages and cell counts for $CD138^+$ cells. Black bars, *Roquin*$^{san/san}$ mice; white bars, $Il27ra^{-/-}Roquin^{san/san}$ mice. Data are pooled from at least three independent experiments and are shown as mean ± SEM. The p values were determined using the unpaired two-tailed Student t test.

total B220$^+$ cells remained similar, although the absolute number was diminished, corresponding with reduced splenomegaly (Fig. 2G). In addition, we investigated the plasma cell populations in these mice. An ~2-fold higher percentage of CD138$^+$ plasma cells (these were also Ig$^+$, data not shown) was observed in *Il27ra*$^{-/-}$*Roquin*$^{san/san}$ mice compared with *Il27ra*$^{+/+}$*Roquin*$^{san/san}$ mice; however, the numbers of plasma cells/spleen were not significantly different (Fig. 2H). These data indicate that IL-27 plays a nonredundant role in GC activity and in the progression of disease in the *sanroque* model.

Altered Ab isotype usage in Il27ra$^{-/-}$Roquin$^{san/san}$ *mice*

IgG2a (IgG2c in C57BL6 mice) is the most pathogenic isotype in murine lupus as a result of its potent ability to activate complement and high-affinity binding to activating Fc receptors (33, 34). Altered Ig isotype usage was observed within the GC B cell gate in

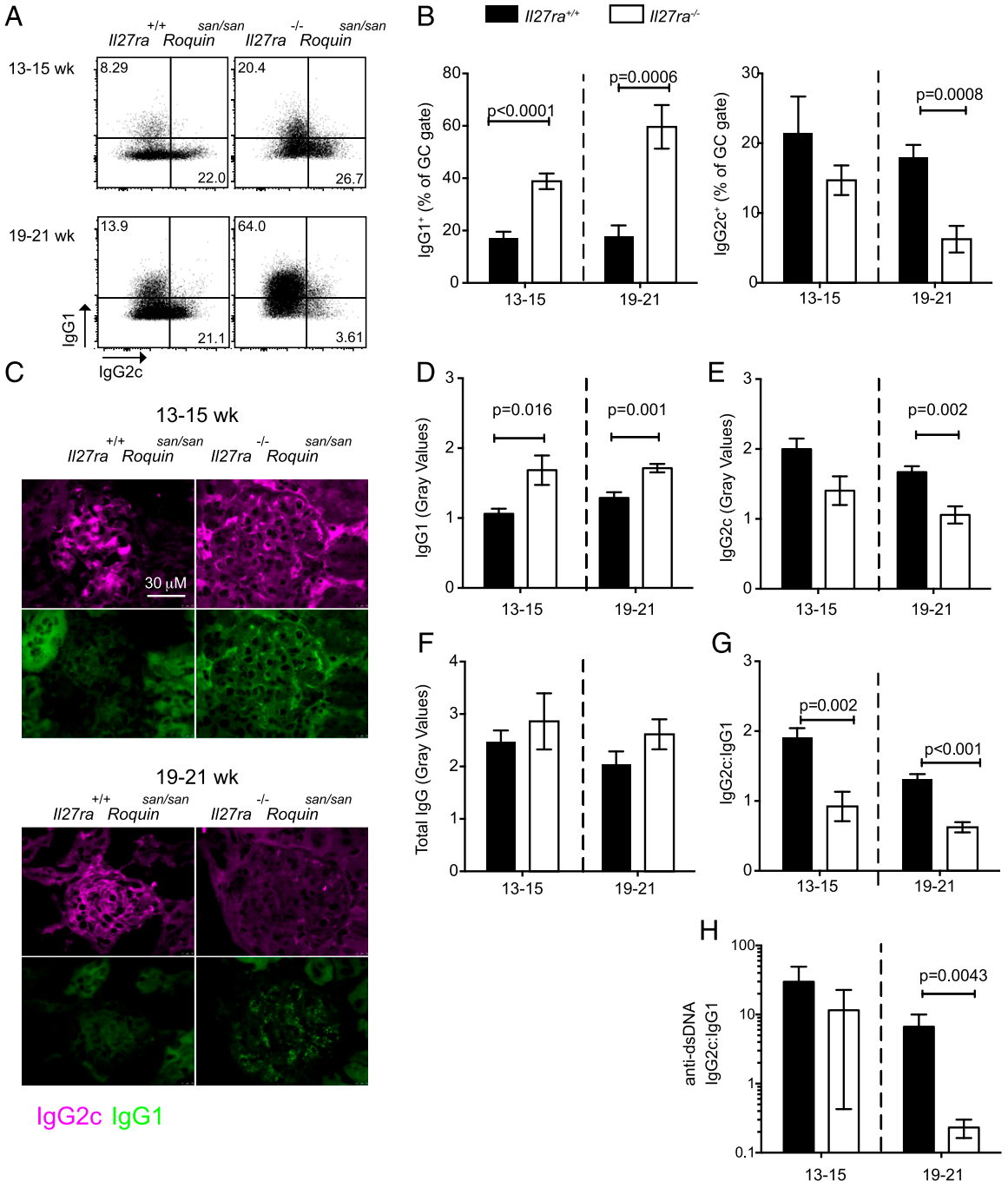

FIGURE 3. Isotype switching and Ig immune complex deposition in the kidneys of *Il27ra*$^{-/-}$*Roquin*$^{san/san}$ mice. (**A** and **B**) Splenocytes from *Il27ra*$^{+/+}$*Roquin*$^{san/san}$ and *Il27ra*$^{-/-}$*Roquin*$^{san/san}$ mice were assessed by flow cytometry. IgG1 and IgG2c surface isotype staining was determined within the GC B cell gate (B220$^+$GL-7$^+$CD38^{lo}). (A) Representative plots. (B) Percentages of cells switched to each isotype at the ages indicated (n = 6–9). (**C**) Representative microscopic images of IgG1 and IgG2a(c) deposition in the kidneys of 13–15-wk-old and 19–21-wk-old *Il27ra*$^{+/+}$*Roquin*$^{san/san}$ and *Il27ra*$^{-/-}$*Roquin*$^{san/san}$ mice. (**D**–**F**) Semiquantified data of immunofluorescent Ig deposition. (D) IgG1 alone. (E) IgG2c alone. (F) Total IgG. (**G**) Ratio of IgG2c/IgG1. (**H**) Serum anti-dsDNA ELISA was performed for isotypes IgG1 and IgG2c. The ratio of anti-dsDNA IgG2c/IgG1 is shown. Data are mean ± SEM (n = 6–7). Black bars, *Il27ra*$^{+/+}$*Roquin*$^{san/san}$ mice; white bars, *Il27ra*$^{-/-}$*Roquin*$^{san/san}$ mice. The p values were determined using the unpaired two-tailed Student t test (B–G) or the Mann–Whitney nonparametric test (H).

the absence of *Il27ra* in *Roquin*$^{san/san}$ mice, with an increase in the percentage of GC B cells switching to IgG1 and fewer cells switching to IgG2a(c) (Fig. 3A, 3B). Importantly, Ig deposits in the kidneys of *Il27ra*$^{-/-}$*Roquin*$^{san/san}$ mice also showed a significant divergence toward IgG1 and away from IgG2a(c) (Fig. 3C–E, 3G), although total Ig deposition was similar (Fig. 3F). This preference for IgG1 over IgG2a(c) in the absence of IL-27 signals was also evident in serum anti-dsDNA Ab levels. Although absolute anti-dsDNA Ab levels were more variable between mice, the ratio of IgG2a:IgG1 in each mouse indicates a clear and significant preference for IgG1 in the absence of IL-27R in aged mice (Fig. 3H). Collectively, the data indicate that IL-27 favors switching to IgG2a(c), an isotype that is central to disease pathogenesis in murine lupus.

IL-27 directly modulates GC B cell activity in the sanroque *spontaneous GC model*

To test whether the reduction in spontaneous GC B cells in *Il27ra*$^{-/-}$*Roquin*$^{san/san}$ mice is influenced by IL-27 signals directly to B cells or occurs secondary to the previously described T_{FH} cell deficiency, we generated congenically marked BM chimeras using equal numbers of cells from CD45.1 *Il27ra*$^{+/+}$*Roquin*$^{san/san}$ and CD45.2 *Il27ra*$^{-/-}$*Roquin*$^{san/san}$ donors. Fifteen weeks after reconstitution, the total B220$^+$ gate was composed of similar percentages of CD45.1 *Il27ra*$^{+/+}$*Roquin*$^{san/san}$ and CD45.2 *Il27ra*$^{-/-}$*Roquin*$^{san/san}$ cells (Fig. 4A). However, when analysis was restricted to GL7$^+$CD38^{lo} GC B cells, there was a significant bias toward *Il27ra*-sufficient cells (Fig. 4B), indicating a B cell–intrinsic defect in the GC in the absence of IL-27Ra. The MFI of CD95 was slightly, but significantly, higher on *Il27ra*-sufficient total B220$^+$ cells, reflecting the increased percentage of GC B cells in the CD45.1 *Il27ra*$^{+/+}$*Roquin*$^{san/san}$ compartment (Supplemental Fig. 3D). In support of this, CD95 MFI within the GC gate was similar between *Il27*ra-sufficient and -deficient cells (Supplemental Fig. 3E). These observations indicate a B cell–intrinsic role for IL-27 in directing B cells toward GC participation.

Interestingly, when Ig isotype switching within the GC B cell gate was examined in mixed chimeric mice, similar percentages of IgG1-expressing cells were observed in the CD45.1 *Il27ra*$^{+/+}$*Roquin*$^{san/san}$ and CD45.2 *Il27ra*$^{-/-}$*Roquin*$^{san/san}$ compartments (Fig. 4D). Also, rather than the expected reduction in IgG2a(c)$^+$ cells in the CD45.2 *Il27ra*$^{-/-}$ gate, there was a small, but significant, increase (Fig. 4D). Thus, changes in isotype switching in the absence of IL-27 signaling are predominantly dictated by B cell–extrinsic factors.

CD4$^+$ T cell–intrinsic effects of IL-27 influence T cell number and IFN-γ production, which may indirectly modify isotype switching in GC B cells

In line with our previous findings (11), chimeric mice displayed a cell-intrinsic defect in CXCR5$^+$PD1$^+$ T_{FH} cells (Fig. 5A). There was also a reduction in the total pool of *Il27ra*$^{-/-}$*Roquin*$^{san/san}$ CD4$^+$ T cells (Fig. 5B). This may reflect the known ability of IL-27 to support the survival of activated CD4$^+$ cells (35) since in this model, a large proportion of cells are CD44$^+$ (~70–80%, data not shown). Consistent with this, we saw a significant reduction in CD44$^+$ cells in the CD4$^+$ T cell compartment of CD45.2$^+$ *Il27ra*$^{-/-}$ cells compared with CD45.1$^+$*Il27ra*$^{+/+}$ cells within the same host mice (data not shown).

IL-27 promotes expression of ICOS (16), a Roquin1 target that is overexpressed in *sanroque* mice and contributes to the disease pathogenesis in this model (36). ICOS levels were significantly

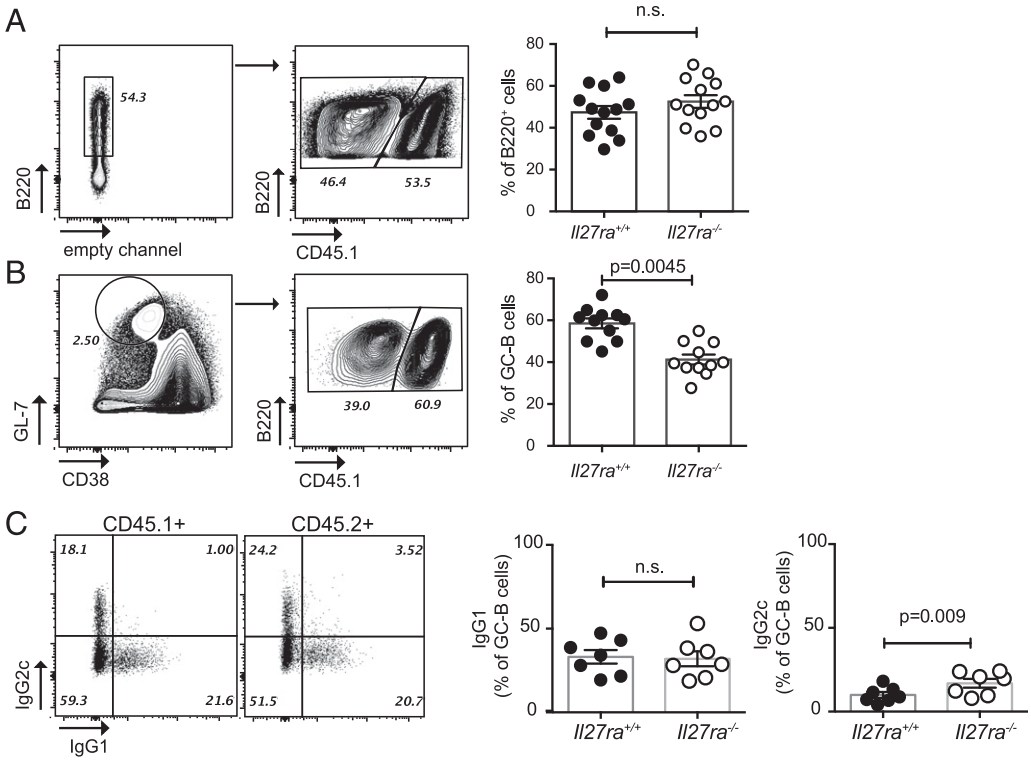

FIGURE 4. B cell–intrinsic and –extrinsic mechanisms contribute to immune deviations in *Il27ra*$^{-/-}$*Roquin*$^{san/san}$ mice. BM cells from *Il27ra*$^{+/+}$*Roquin*$^{san/san}$ (CD45.1) and *Il27ra*$^{-/-}$*Roquin*$^{san/san}$ (CD45.2) mice were mixed in a 1:1 ratio and injected into previously irradiated *Rag1*$^{-/-}$ mice. At 15 wk postreconstitution, spleen was harvested and assessed by flow cytometry for the percentages of CD45.1 *Il27ra*$^{+/+}$ and CD45.2 *Il27ra*$^{-/-}$ cells in total B220$^+$ cells (**A**) and B220$^+$, GL-7$^+$CD38^{lo} GC B cells (**B**). (**C**) Percentages of IgG1 versus IgG2a(c) switched cells within the GC compartment of CD45.1$^+$ and CD45.2$^+$ cells. Symbols represent individual mice. Bars represent mean ± SEM. Similar results were observed in three independent experiments. The *p* values were determined using the paired two-tailed Student *t* test. n.s., not significant.

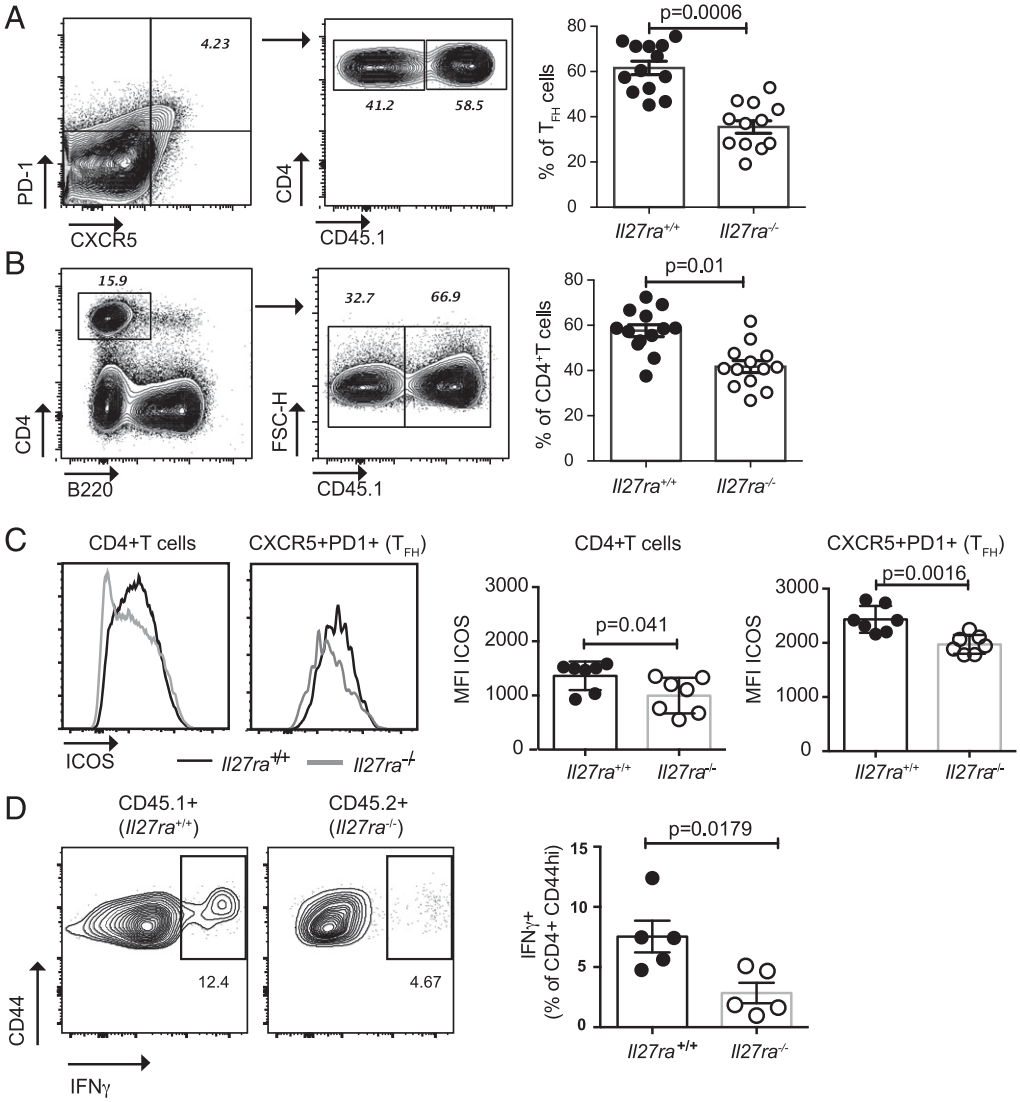

FIGURE 5. T cell–intrinsic immune deviations in *Il27ra*$^{-/-}$*Roquin*$^{san/san}$ mice. BM cells from *Il27ra*$^{+/+}$*Roquin*$^{san/san}$ (CD45.1) and *Il27ra*$^{-/-}$*Roquin*$^{san/san}$ (CD45.2) mice were mixed in a 1:1 ratio and injected into previously irradiated *Rag1*$^{-/-}$ mice. At 15 wk postreconstitution, spleen was harvested and assessed by flow cytometry to determine the percentages of CD45.1 *Il27ra*$^{+/+}$ and CD45.2 *Il27ra*$^{-/-}$ cells in various cellular compartments. (**A**) PD1^{+} CXCR5^{+} cells (within the CD4^{+}B220^{-} gate). (**B**) Total CD4^{+}B220^{-} cells. (**C**) ICOS MFI within the CD45.1 (Il27ra$^{+/+}$) and CD45.2 (Il27ra$^{-/-}$) compartments of total CD4^{+}B220^{-} cells or CD4^{+}B220^{-}CXCR5^{+}PD1^{+} (T_{FH}) gates. (**D**) Cells harvested from chimeric mice were stimulated with PMA and ionomycin for 4 h in vitro before intracellular staining to detect IFN-γ. CD4^{+}CD44^{+} cells were gated and the genotype was determined based on CD45.1 or CD45.2 expression before analyzing the percentage of IFN-γ^{+} cells in each compartment. Symbols represent individual mice. Bars represent mean ± SEM. Similar results were observed in two independent experiments. The *p* values were determined using the paired two-tailed Student *t* test.

reduced in the absence of *Il27ra* within the total CD4^{+} pool, as well as within the CXCR5^{+}PD1^{+}CD4^{+} T_{FH} cell gate (Fig. 5C).

IFN-γ is a target of Roquin1 and a key mediator of disease in the *sanroque* lupus model, promoting T_{FH} cell accumulation (26). IFN-γ also stimulates IgG2a isotype switching in B cells (37). IL-27 is a key regulator of Th cell polarization and is known to upregulate IFN-γ expression by CD4^{+} T cells (4). Intracellular cytokine staining of chimeric splenocytes revealed that fewer CD4^{+}CD44^{+} T_{FH}-like cells produced IFN-γ in the absence of *Il27ra* (Fig. 5D).

Discussion

There is growing evidence that IL-27 can support Ab-driven autoimmune disease. Studies of untreated SLE patients found that IL-27 was significantly elevated in the sera compared with healthy controls (9, 10). Interestingly, glucocorticoids, which are commonly used to treat SLE, significantly suppress IL-27 production (9). The reduction in serum IL-27 during immunosuppressive therapy may influence the results of studies in which treated patients were not excluded. In several such studies, IL-27 in patient sera was diminished or not significantly different from healthy controls (38–40). An essential role for IL-27 in murine lupus is indicated by several studies. We previously observed reduced GCs, anti-nuclear Abs, and nephritis in *Il27ra*-deficient mice in pristane-driven lupus (11). Deletion of *Il27ra*, or IL-27 subunit *Ebi3*, in MLR/*lpr* lupus-prone mice resulted in altered disease pathology and prolonged survival (12, 13), although an associated skin inflammation was exacerbated in the absence of *Il27ra* (41). In this study, we used the *Roquin*$^{san/san}$ mouse model, in which spontaneous GCs drive disease, and report that IL-27R deficiency reduced disease severity. Together, these data point to a role for IL-27 in promoting high-affinity Ab production in autoimmune disease.

Although B cells were shown to express IL-27R and undergo STAT1 and STAT3 activation in response to IL-27 stimulation, the

functional role of IL-27 signals to B cells has remained unclear. On one hand, B cell development and basal serum Ig are normal (with the exception of IgG2a) in *Il27ra*$^{-/-}$ mice. On the other hand, high-affinity Ab responses are diminished by the loss of IL-27 signals (4, 11). The data presented in this article demonstrate that IL-27 specifically promotes STAT1-dependent differentiation of CD20^{+} CD38^{+}CD10^{+}CD95^{+}CD27^{lo} B cells, but not plasma cells, and that B cell–intrinsic effects of IL-27 are required to sustain the expansion of GC B cells in the *sanroque* autoimmune disease model.

The *Il27ra*$^{-/-}$*Roquin*$^{san/san}$ BM chimera experiments revealed a B cell–intrinsic requirement for IL-27 during GC responses in vivo. *Il27ra*-deficient *sanroque* GC B cells were reduced significantly compared with *Il27ra*-sufficient cells within the same host mouse. In *Il27ra*$^{-/-}$*Roquin*$^{san/san}$ mice, cells that entered the GC had normal proportions of light and dark zone cells, suggesting that IL-27 acts prior to GC commitment or is equally important at each stage of the GC.

IL-27 stimulation of human B cells in vitro resulted in enhanced differentiation of cells with a GC-like phenotype expressing CD38, CD20, CD95, and CD10. Because Bcl-6 was lost from all B cell cultures, including bona fide in vivo–generated tonsillar GC B cells, we reason that the requirements for Bcl-6 maintenance are not recreated in these B cell–only cultures. Therefore, it is difficult to draw conclusions about the effect of IL-27 in this regard. Upregulation of CD95 in response to IL-27 stimulation was observed but was not associated with changes in cell survival or proliferation. IL-27 can upregulate B cell expression of ICAM-1 and CD86 (20), molecules that promote productive interactions with T cells, and also promote GC activity in an in vivo context (42). The coordinated upregulation of these GC markers, with no alteration in cell proliferation or survival, suggest that IL-27–induced STAT1 signals alter the B cell–differentiation program.

Although the ability of IL-27 to support T_{FH} cell activity in humans and mice is dependent on STAT3 (11, 15, 35, 43), we found that its ability to enhance GC B cell marker expression is reliant on STAT1 (Fig. 1). The reduced ability of $STAT1_{MUT}$ naive B cells to upregulate GC cell surface markers in response to IL-27 is not indicative of a generalized defect in activation, because we previously demonstrated that these cells undergo normal plasmablast differentiation in response to IL-21 in vitro (32, 44).

In mouse B cells, in vitro rIL-27–induced STAT1 activation altered class switching away from IgG1 and toward IgG2a (21). Likewise, we observed that IgG1 was increased and IgG2a(c) was decreased in *Il27ra*-deficient *Roquin*$^{san/san}$ mice. However, BM chimeras revealed that Ig isotype usage was dominated by B cell–extrinsic signals. Moreover, addition of rIL-27 to human B cells cultured in the presence of rIL-21 to induce plasmablast formation did not influence Ig isotype switching. The reduction that we observed in IFN-γ production by *Il27ra*$^{-/-}$ T cells in this model could provide a B cell–extrinsic mechanism for reduced IgG2a(c). IFN-γ promotes IgG2a(c) and inhibits IL-4–induced IgG1 (37). The Th1-promoting and Th2-suppressing abilities of IL-27 are well characterized (4, 5). We noted that isotype switching was affected within the B220^{+}GL7^{+}CD38^{lo} GC B cell gate in *Il27ra*$^{-/-}$*Roquin*$^{san/san}$ mice. This suggests that cytokine changes are present within the GC or that cytokine signaling before GC entry alters isotype switching. However, altered isotype switching in extrafollicular B cells may also contribute.

The altered isotype usage is likely to contribute to the amelioration of disease in *Il27ra*$^{-/-}$*Roquin*$^{san/san}$ mice. In *Il27ra*$^{-/-}$ *Roquin*$^{san/san}$ mice, as well as in studies that examined the effect of *Il27ra* deficiency in other models of autoimmunity (12–14), the loss of IL-27 signaling consistently skewed isotype switching away from pathogenic IgG2a(c) and toward IgG1. There is a preponderance of IgG2a in murine lupus models, and IgG2 isotypes are the most pathogenic subclasses in vivo because of their ability to engage high-affinity FcγRIV, whereas IgG1 Abs are significantly less pathogenic because they preferentially engage the inhibitory FcγRIIB and are unable to activate complement by the classical pathway (33, 34). Moreover, murine IgG1 was recently shown to be protective in a model of nephritic immune complex deposition as a result of its ability to destabilize self-associating IgG3 complexes (45).

It should be noted that overexpression of IL-27Rα was shown to protect against various features of disease in the MRL/*lpr* lupus model (41, 46). These findings may stem from the well-established immunosuppressive properties of IL-27 on T cells (5) and, in the context of unusually high levels of signaling, those suppressive effects evidently dominate. Our data suggest that physiological levels of IL-27 signaling are required to promote GC B and T_{FH} cell activity, without inhibiting the GC response.

As summarized in Supplemental Fig. 4, IL-27 influences multiple parameters that are pertinent to GC activity and lupus progression. *Il27ra*$^{-/-}$*Roquin*$^{san/san}$ mice had defects intrinsic to both GC B and T_{FH} cells. Roquin1 facilitates the degradation of ICOS and IFN-γ mRNAs, which are central to disease pathogenesis in this model (26, 36, 47) and are regulated by IL-27 (5). Loss of IL-27 signaling resulted in lower frequencies of IFN-γ–producing CD4^{+} T cells, as well as diminished expression of ICOS on total CD4^{+} or CD4^{+}PD1^{+}CXCR5^{+} T_{FH} cells. Thus, the impact of IL-27 in this system is the culmination of effects on B and T cells. The data presented illuminate a previously unappreciated role for IL-27 in directly promoting GC B cell activity and highlight a B cell–intrinsic requirement for IL-27 during GC responses in a mouse model of autoimmunity.

Acknowledgments

We thank the STAT3- and STAT1-deficient patients for their valuable contribution to this project, the Garvan Institute Flow Cytometry Facility for cell sorting, and the Garvan Institute Biological Testing Facility and Animal BioResources Australia for animal husbandry.

Disclosures

N.G. is a full-time employee of Genentech, a member of the Roche group. He also holds stock in Roche, Novartis, and Novo Nordisk. The other authors have no financial conflicts of interest.

References

1. Brink, R. 2014. The imperfect control of self-reactive germinal center B cells. *Curr. Opin. Immunol.* 28: 97–101.
2. Tangye, S. G., C. S. Ma, R. Brink, and E. K. Deenick. 2013. The good, the bad and the ugly - TFH cells in human health and disease. *Nat. Rev. Immunol.* 13: 412–426.
3. Vinuesa, C. G., I. Sanz, and M. C. Cook. 2009. Dysregulation of germinal centres in autoimmune disease. *Nat. Rev. Immunol.* 9: 845–857.
4. Yoshida, H., and C. A. Hunter. 2015. The immunobiology of interleukin-27. *Annu. Rev. Immunol.* 33: 417–443.
5. Hall, A. O., J. S. Silver, and C. A. Hunter. 2012. The immunobiology of IL-27. *Adv. Immunol.* 115: 1–44.
6. Batten, M., J. Li, S. Yi, N. M. Kljavin, D. M. Danilenko, S. Lucas, J. Lee, F. J. de Sauvage, and N. Ghilardi. 2006. Interleukin 27 limits autoimmune encephalomyelitis by suppressing the development of interleukin 17-producing T cells. *Nat. Immunol.* 7: 929–936.
7. Diveu, C., M. J. McGeachy, K. Boniface, J. S. Stumhofer, M. Sathe, B. Joyce-Shaikh, Y. Chen, C. M. Tato, T. K. McClanahan, R. de Waal Malefyt, et al. 2009. IL-27 blocks RORc expression to inhibit lineage commitment of Th17 cells. *J. Immunol.* 182: 5748–5756.
8. Murugaiyan, G., and B. Saha. 2013. IL-27 in tumor immunity and immunotherapy. *Trends Mol. Med.* 19: 108–116.
9. Qiu, F., L. Song, N. Yang, and X. Li. 2013. Glucocorticoid downregulates expression of IL-12 family cytokines in systemic lupus erythematosus patients. *Lupus* 22: 1011–1016.
10. Xia, L. P., B. F. Li, H. Shen, and J. Lu. 2015. Interleukin-27 and interleukin-23 in patients with systemic lupus erythematosus: possible role in lupus nephritis. *Scand. J. Rheumatol.* 44: 200–205.

11. Batten, M., N. Ramamoorthi, N. M. Kljavin, C. S. Ma, J. H. Cox, H. S. Dengler, D. M. Danilenko, P. Caplazi, M. Wong, D. A. Fulcher, et al. 2010. IL-27 supports germinal center function by enhancing IL-21 production and the function of T follicular helper cells. *J. Exp. Med.* 207: 2895–2906.
12. Igawa, T., H. Nakashima, A. Sadanaga, K. Masutani, K. Miyake, S. Shimizu, A. Takeda, S. Hamano, and H. Yoshida. 2009. Deficiency in EBV-induced gene 3 (EBI3) in MRL/lpr mice results in pathological alteration of autoimmune glomerulonephritis and sialadenitis. *Mod. Rheumatol.* 19: 33–41.
13. Shimizu, S., N. Sugiyama, K. Masutani, A. Sadanaga, Y. Miyazaki, Y. Inoue, M. Akahoshi, R. Katafuchi, H. Hirakata, M. Harada, et al. 2005. Membranous glomerulonephritis development with Th2-type immune deviations in MRL/lpr mice deficient for IL-27 receptor (WSX-1). *J. Immunol.* 175: 7185–7192.
14. Cao, Y., P. D. Doodes, T. T. Glant, and A. Finnegan. 2008. IL-27 induces a Th1 immune response and susceptibility to experimental arthritis. *J. Immunol.* 180: 922–930.
15. Harker, J. A., A. Dolgoter, and E. I. Zuniga. 2013. Cell-intrinsic IL-27 and gp130 cytokine receptor signaling regulates virus-specific CD4$^+$ T cell responses and viral control during chronic infection. *Immunity* 39: 548–559.
16. Pot, C., H. Jin, A. Awasthi, S. M. Liu, C. Y. Lai, R. Madan, A. H. Sharpe, C. L. Karp, S. C. Miaw, I. C. Ho, and V. K. Kuchroo. 2009. Cutting edge: IL-27 induces the transcription factor c-Maf, cytokine IL-21, and the costimulatory receptor ICOS that coordinately act together to promote differentiation of IL-10-producing Tr1 cells. *J. Immunol.* 183: 797–801.
17. Ma, C. S., D. T. Avery, A. Chan, M. Batten, J. Bustamante, S. Boisson-Dupuis, P. D. Arkwright, A. Y. Kreins, D. Averbuch, D. Engelhard, et al. 2012. Functional STAT3 deficiency compromises the generation of human T follicular helper cells. *Blood* 119: 3997–4008.
18. Gringhuis, S. I., T. M. Kaptein, B. A. Wevers, M. van der Vlist, E. J. Klaver, I. van Die, L. E. Vriend, M. A. de Jong, and T. B. Geijtenbeek. 2014. Fucose-based PAMPs prime dendritic cells for follicular T helper cell polarization via DC-SIGN-dependent IL-27 production. *Nat. Commun.* 5: 5074.
19. Cocco, C., F. Morandi, and I. Airoldi. 2011. Interleukin-27 and interleukin-23 modulate human plasmacell functions. *J. Leukoc. Biol.* 89: 729–734.
20. Larousserie, F., P. Charlot, E. Bardel, J. Froger, R. A. Kastelein, and O. Devergne. 2006. Differential effects of IL-27 on human B cell subsets. *J. Immunol.* 176: 5890–5897.
21. Yoshimoto, T., K. Okada, N. Morishima, S. Kamiya, T. Owaki, M. Asakawa, Y. Iwakura, F. Fukai, and J. Mizuguchi. 2004. Induction of IgG2a class switching in B cells by IL-27. *J. Immunol.* 173: 2479–2485.
22. Chen, Q., N. Ghilardi, H. Wang, T. Baker, M. H. Xie, A. Gurney, I. S. Grewal, and F. J. de Sauvage. 2000. Development of Th1-type immune responses requires the type I cytokine receptor TCCR. *Nature* 407: 916–920.
23. Vinuesa, C. G., M. C. Cook, C. Angelucci, V. Athanasopoulos, L. Rui, K. M. Hill, D. Yu, H. Domaschenz, B. Whittle, T. Lambe, et al. 2005. A RING-type ubiquitin ligase family member required to repress follicular helper T cells and autoimmunity. *Nature* 435: 452–458.
24. Linterman, M. A., R. J. Rigby, R. Wong, D. Silva, D. Withers, G. Anderson, N. K. Verma, R. Brink, A. Hutloff, C. C. Goodnow, and C. G. Vinuesa. 2009. Roquin differentiates the specialized functions of duplicated T cell costimulatory receptor genes CD28 and ICOS. *Immunity* 30: 228–241.
25. Linterman, M. A., R. J. Rigby, R. K. Wong, D. Yu, R. Brink, J. L. Cannons, P. L. Schwartzberg, M. C. Cook, G. D. Walters, and C. G. Vinuesa. 2009. Follicular helper T cells are required for systemic autoimmunity. *J. Exp. Med.* 206: 561–576.
26. Lee, S. K., D. G. Silva, J. L. Martin, A. Pratama, X. Hu, P. P. Chang, G. Walters, and C. G. Vinuesa. 2012. Interferon-γ excess leads to pathogenic accumulation of follicular helper T cells and germinal centers. *Immunity* 37: 880–892.
27. Pratama, A., R. R. Ramiscal, D. G. Silva, S. K. Das, V. Athanasopoulos, J. Fitch, N. K. Botelho, P. P. Chang, X. Hu, J. J. Hogan, et al. 2013. Roquin-2 shares functions with its paralog Roquin-1 in the repression of mRNAs controlling T follicular helper cells and systemic inflammation. *Immunity* 38: 669–680.
28. Yu, D., S. Rao, L. M. Tsai, S. K. Lee, Y. He, E. L. Sutcliffe, M. Srivastava, M. Linterman, L. Zheng, N. Simpson, et al. 2009. The transcriptional repressor Bcl-6 directs T follicular helper cell lineage commitment. *Immunity* 31: 457–468.
29. Vogel, K. U., S. L. Edelmann, K. M. Jeltsch, A. Bertossi, K. Heger, G. A. Heinz, J. Zöller, S. C. Warth, K. P. Hoefig, C. Lohs, et al. 2013. Roquin paralogs 1 and 2 redundantly repress the Icos and Ox40 costimulator mRNAs and control follicular helper T cell differentiation. *Immunity* 38: 655–668.
30. Avery, D. T., E. K. Deenick, C. S. Ma, S. Suryani, N. Simpson, G. Y. Chew, T. D. Chan, U. Palendira, J. Bustamante, S. Boisson-Dupuis, et al. 2010. B cell-intrinsic signaling through IL-21 receptor and STAT3 is required for establishing long-lived antibody responses in humans. *J. Exp. Med.* 207: 155–171.
31. Galibert, L., N. Burdin, B. de Saint-Vis, P. Garrone, C. Van Kooten, J. Banchereau, and F. Rousset. 1996. CD40 and B cell antigen receptor dual triggering of resting B lymphocytes turns on a partial germinal center phenotype. *J. Exp. Med.* 183: 77–85.
32. Tangye, S. G., D. T. Avery, E. K. Deenick, and P. D. Hodgkin. 2003. Intrinsic differences in the proliferation of naive and memory human B cells as a mechanism for enhanced secondary immune responses. *J. Immunol.* 170: 686–694.
33. Nimmerjahn, F., P. Bruhns, K. Horiuchi, and J. V. Ravetch. 2005. FcgammaRIV: a novel FcR with distinct IgG subclass specificity. *Immunity* 23: 41–51.
34. Nimmerjahn, F., and J. V. Ravetch. 2008. Fcgamma receptors as regulators of immune responses. *Nat. Rev. Immunol.* 8: 34–47.
35. Kim, G., R. Shinnakasu, C. J. Saris, H. Cheroutre, and M. Kronenberg. 2013. A novel role for IL-27 in mediating the survival of activated mouse CD4 T lymphocytes. *J. Immunol.* 190: 1510–1518.
36. Yu, D., A. H. Tan, X. Hu, V. Athanasopoulos, N. Simpson, D. G. Silva, A. Hutloff, K. M. Giles, P. J. Leedman, K. P. Lam, et al. 2007. Roquin represses autoimmunity by limiting inducible T-cell co-stimulator messenger RNA. *Nature* 450: 299–303.
37. Snapper, C. M., and W. E. Paul. 1987. Interferon-gamma and B cell stimulatory factor-1 reciprocally regulate Ig isotype production. *Science* 236: 944–947.
38. Li, T. T., T. Zhang, G. M. Chen, Q. Q. Zhu, J. H. Tao, H. F. Pan, and D. Q. Ye. 2010. Low level of serum interleukin 27 in patients with systemic lupus erythematosus. *J. Investig. Med.* 58: 737–739.
39. Duarte, A. L., A. T. Dantas, H. de Ataíde Mariz, F. A. dos Santos, J. C. da Silva, L. F. da Rocha, Jr., S. L. Galdino, and M. Galdino da Rocha Pitta. 2013. Decreased serum interleukin 27 in Brazilian systemic lupus erythematosus patients. *Mol. Biol. Rep.* 40: 4889–4892.
40. Kwan, B. C., L. S. Tam, K. B. Lai, F. M. Lai, E. K. Li, G. Wang, K. M. Chow, P. K. Li, and C. C. Szeto. 2009. The gene expression of type 17 T-helper cell-related cytokines in the urinary sediment of patients with systemic lupus erythematosus. *Rheumatology (Oxford)* 48: 1491–1497.
41. Kido, M., S. Takeuchi, N. Sugiyama, H. Esaki, H. Nakashima, H. Yoshida, and M. Furue. 2011. T cell-specific overexpression of interleukin-27 receptor α subunit (WSX-1) prevents spontaneous skin inflammation in MRL/lpr mice. *Br. J. Dermatol.* 164: 1214–1220.
42. Dennig, D., J. Lacerda, Y. Yan, C. Gasparetto, and R. J. O'Reilly. 1994. ICAM-1 (CD54) expression on B lymphocytes is associated with their costimulatory function and can be increased by coactivation with IL-1 and IL-7. *Cell. Immunol.* 156: 414–423.
43. Ysebrant de Lendonck, L., F. Eddahri, Y. Delmarcelle, M. Nguyen, O. Leo, S. Goriely, and A. Marchant. 2013. STAT3 signaling induces the differentiation of human ICOS(+) CD4 T cells helping B lymphocytes. *PLoS One* 8: e71029.
44. Deenick, E. K., D. T. Avery, A. Chan, L. J. Berglund, M. L. Ives, L. Moens, J. L. Stoddard, J. Bustamante, S. Boisson-Dupuis, M. Tsumura, et al. 2013. Naive and memory human B cells have distinct requirements for STAT3 activation to differentiate into antibody-secreting plasma cells. *J. Exp. Med.* 210: 2739–2753.
45. Strait, R. T., M. T. Posgai, A. Mahler, N. Barasa, C. O. Jacob, J. Köhl, M. Ehlers, K. Stringer, S. K. Shanmukhappa, D. Witte, et al. 2015. IgG1 protects against renal disease in a mouse model of cryoglobulinaemia. *Nature* 517: 501–504.
46. Sugiyama, N., H. Nakashima, T. Yoshimura, A. Sadanaga, S. Shimizu, K. Masutani, T. Igawa, M. Akahoshi, K. Miyake, A. Takeda, et al. 2008. Amelioration of human lupus-like phenotypes in MRL/lpr mice by overexpression of interleukin 27 receptor alpha (WSX-1). *Ann. Rheum. Dis.* 67: 1461–1467.
47. Chang, P. P., S. K. Lee, X. Hu, G. Davey, G. Duan, J. H. Cho, G. Karupiah, J. Sprent, W. R. Heath, E. M. Bertram, and C. G. Vinuesa. 2012. Breakdown in repression of IFN-γ mRNA leads to accumulation of self-reactive effector CD8+ T cells. *J. Immunol.* 189: 701–710.